

Orientation-Independent Charge Transport in Single Spherulites from Solution-Processed Organic Semiconductors

Stephanie S. Lee,[†] Marsha A. Loth,[‡] John E. Anthony,[‡] and Yueh-Lin Loo^{*,†}

[†]Department of Chemical and Biological Engineering, Princeton University, Princeton, New Jersey 08544, United States

[‡]Department of Chemistry, University of Kentucky, Lexington, Kentucky 40506, United States

ABSTRACT: Due to the rapidity of morphological development during deposition, solution-processed organic semiconductor thin films exist in semicrystalline or polycrystalline states, incorporating a high degree of local variations in molecular orientation compared to their single-crystal counterparts. Spherulites, a common crystalline superstructure found in these systems, for example, incorporate a large distribution of molecular orientations about the radial axis to maintain their space-filling growth habit. Here, we aim to determine how this distribution of molecular orientations influences charge transport by fabricating arrays of devices on single spherulites. Given that the orientation distribution that is present about the radial axis mandates the presence of low-angle grain boundaries within single spherulites, we find intraspherulitic charge transport to be independent of the general direction of π -stacking; organic field-effect transistors exhibit comparable mobilities regardless of how their channels are oriented with respect to the general π -stacking direction.

Much of our understanding of the intrinsic charge transport properties of organic semiconductors originates from studies of single crystals. Although exceedingly slow growth (often between 24 and 48 h) and requirements for high-purity starting materials¹ restrict the usefulness of single crystals for commercial applications, the absence of grain boundaries and the presence of near-perfect molecular ordering in these materials make them ideal for examining the efficacy of charge transport along different molecular orientations.^{2–7} Single-crystal organic field-effect transistors (OFETs) made by soft-contact lamination, for example, have been reported to exhibit the highest mobility when the active channels are coincident with the direction of maximum π -orbital overlap in rubrene.⁴ This and other single-crystal studies^{2–7} have conclusively shown charge transport to be anisotropic along different crystallographic planes, correlated with the details of molecular orientation.

While these studies shed light on fundamental charge transport, they may not necessarily translate to application-relevant, solution-processed organic semiconductor thin films that are often polycrystalline and spherulitic.⁸ The structure of spherulites, in particular, is hierarchical in nature and incorporates heterogeneities due to molecular orientation mismatch on multiple length scales. At the micrometer to millimeter length scale, high-angle interspherulitic boundaries exist where neighboring spherulites impinge; these boundaries

can act as macroscopic barriers to charge transport.^{9,10} Critical to the space-filling growth of individual spherulites, a distribution of molecular orientations about the radial axis exists at the nanometer length scale.¹¹ A single spherulite thus effectively comprises many smaller grains that are separated by low-angle intraspherulite grain boundaries, with the growth of these grains directed radially from its nucleation point. To this end, spherulites, given their broad but quantifiable distribution of local molecular orientations about the radial axis, present a unique opportunity to elucidate how molecular orientation distribution, and thus the presence of low-angle grain boundaries, impacts the anticipated charge transport anisotropy reported along the different crystallographic planes in organic semiconductor single crystals.

Although spherulites incorporate a distribution of molecular orientations, it is in fact possible to define a general direction of maximum π -orbital overlap relative to the center of the spherulite. Our study begins with solution-processable triethylsilylethynyl anthradithiophene (TES ADT). Solvent-vapor annealing of predeposited thin films routinely results in millimeter-sized spherulites.¹² Quantitative grazing-incidence X-ray diffraction studies on directionally crystallized TES ADT reveal that its π -stacking direction corresponds closely to the macroscopic radial axis of the growing spherulites, with the mean π -stacking direction tilted $8 \pm 5^\circ$ away from the macroscopic radial axis.¹³ At the X-ray incident angle of 0.16° (corresponding to an angle just below the critical angle of the underlying Si/SiO₂ substrate) that we employ, this measurement reflects the ensemble-average orientation along the depth of TES ADT. Given the charge anisotropies reported in single-crystal organic semiconductors, we expect charge transport to be the fastest along the radial direction of the spherulite, corresponding to the direction of maximum π -orbital overlap. Yet, the space-filling nature of spherulitic growth mandates the presence of a distribution of molecular orientations, and in turn low-angle grain boundaries, about this direction of maximum π -orbital overlap. The judicious placement of source and drain electrodes atop individual spherulites thus allows us to elucidate how this distribution of orientations influences the anticipated mobility anisotropy in OFETs when the mean π -stacking direction of TES ADT is altered with respect to the ideal charge transport direction in the active channels.

TES ADT is first deposited onto SiO₂/Si substrates by spin coating from toluene; this process results in a uniform, 100-nm thick film (experimental methods are detailed elsewhere^{9,13}). Central to this study is the fact that as-cast TES ADT films

Received: December 13, 2011

Published: February 3, 2012

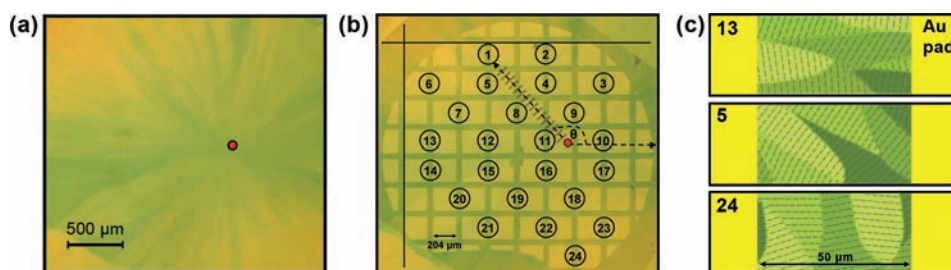


Figure 1. (a) A single TES ADT spherulite, with a red circle indicating the center of the spherulite. (b) The same spherulite with 60-nm thick Au pads evaporated on top. Pairs of Au pads were used as the source and drain electrodes for transistor measurements. Numbers indicate the channel regions of each transistor tested. Dashed lines indicate how θ , the angle between the macroscopic radial axis of the spherulite and the vector defining the charge transport direction for transistor 1, is calculated. Gray lines along the radial axis represent the π -planes of TES ADT. (c) Illustrations of the channel regions of device 13, 5, and 24, showing the general molecular orientation of TES ADT. Lines represent the π -planes of TES ADT.

display only limited ordering,¹³ allowing us to controllably induce further crystallization via subsequent postdeposition exposure of the films to 1,2-dichloroethane (DCE) solvent vapors.^{12,14,15} During exposure to DCE solvent vapors, TES ADT spherulites nucleate, usually on dust particles or defects, and they grow until they impinge one another, easily reaching diameters of >3 mm on clean surfaces. Since the size of the spherulites is 4 orders of magnitude larger than the thickness of TES ADT thin films, we assume the spherulitic morphology persists through the depth of these 100-nm thick films.

Within an individual TES ADT spherulite exists a distribution of orientations to accommodate its space-filling growth habit. This distribution of orientation necessitates the presence of low-angle grain boundaries within single spherulites. We have quantified the distribution of molecular orientations about the mean π -stacking direction by measuring the full-width at half the maximum intensity (fwhm) of φ -scans, in which the intensity of a given X-ray reflection is measured as the sample is rotated in the path of the X-ray beam.¹³ Similar experiments have previously been conducted on rubrene single crystals; the fwhm obtained during such a φ -scan about the (600) reflection is less than 0.02° .⁵ Such a narrow fwhm indicates minimal orientation distribution within the single crystal. By contrast, the φ -scan conducted on the (001) reflection of unidirectionally crystallized poly(3-hexyl thiophene), P3HT, films reveals an fwhm of 10° .¹⁶ This experiment indicates that P3HT samples a much larger distribution of molecular orientations about the polymer-chain axis, even when these films have been preferentially oriented via the application of a temperature gradient. The fwhm of φ -scans conducted on the (122) reflection of unidirectionally crystallized TES ADT, in which spherulitic growth is confined to a narrow channel, is 20° and is twice as large¹³ as that of unidirectionally oriented P3HT films. Compared to single crystals of rubrene and unidirectionally oriented P3HT, TES ADT thus samples a larger distribution of molecular orientations about the macroscopic radial axis when crystallized. Analysis of our φ -scans indicates that the π -planes of neighboring TES ADT grains within a single spherulite can be tilted as much as 20° from the mean π -stacking direction. By probing charge transport at multiple locations within an individual spherulite, we can thus examine, in the presence of such a broad molecular orientation distribution, whether the relative alignment of the mean π -stacking direction of TES ADT and the charge transport direction of transistors affects performance.

To study the impact of having an orientation distribution with an fwhm of 20° about the mean π -stacking direction in the

active layer on OFET device performance, we fabricated an array of electrodes on a single spherulite to act as source and drain electrodes for top-contact, bottom-gate OFET measurements. Figure 1a shows an optical micrograph of a single TES ADT spherulite. The nucleation point of the spherulite is highlighted with a red circle. The color contrast in the optical micrograph reflects the optical birefringence that results from slight orientation mismatches between adjacent intraspherulite grains. We used a transmission electron microscopy (TEM) sample grid as a shadow mask to define 60-nm thick top-contact gold electrodes atop the spherulite (refer to Figure 1b). Previously, we found that depositing top-contact electrodes via electron-beam deposition can damage the underlying TES ADT, leading to degradation in device performance.¹⁴ Here, deposition of gold electrodes is carried out via thermal evaporation to minimize damage to the active layer. The channel regions of 24 devices that were tested are numbered in Figure 1b for clarity. For each device, we define θ as the angle between the macroscopic radial axis of the spherulite, which loosely corresponds to the mean π -stacking direction of TES ADT, and the vector defining the charge transport direction of the transistor. The π -planes corresponding to this mean π -stacking direction are represented by short, gray lines in Figure 1b for clarity. By definition, the mean π -stacking direction of TES ADT is thus generally parallel to the ideal charge transport direction within the active channels of OFETs at $\theta = 0^\circ$, 180° , and 360° (the mean π -stacking direction is tilted by $8 \pm 5^\circ$ relative to the radial axis of the spherulite) and is normal to the ideal charge transport direction when $\theta = 90^\circ$ and 270° . Figure 1c displays illustrations of the channel region of devices 13, 5, and 24, and it articulates the general molecular orientation of TES ADT with respect to the charge transport direction of the respective devices. The black lines represent the π -planes of TES ADT. In the active channel of device 13 (top), for example, TES ADT is generally oriented with its mean π -stacking direction tilted 10° from the charge transport direction of the transistor (so $\theta = 178^\circ$). In the active channel of device 5 (middle), TES ADT is oriented with its mean π -stacking direction tilted 30° away from the desired charge transport direction ($\theta = 128^\circ$), and in the active channel of device 24 (bottom), the mean π -stacking direction is on average normal to the charge transport direction ($\theta = 276^\circ$). Despite the space-filling nature of spherulitic growth, which mandates that a distribution of molecular orientations about the mean π -stacking direction be sampled within the active channels, as illustrated in Figure 1c, the channels of these individual devices comprise TES ADT with a macroscopically distinguishable π -

stacking direction with respect to the ideal charge transport direction of the OFETs.

Based on previous research reports in which charge transport in single crystals is fastest along the π -stacking direction of organic semiconductors,^{2–7} we thus initially expected the mobility of device 5 to be the highest and the mobility of device 24 to be the lowest. Yet, the output and transfer curves (Figure 2) are comparable, suggesting that charge transport across the

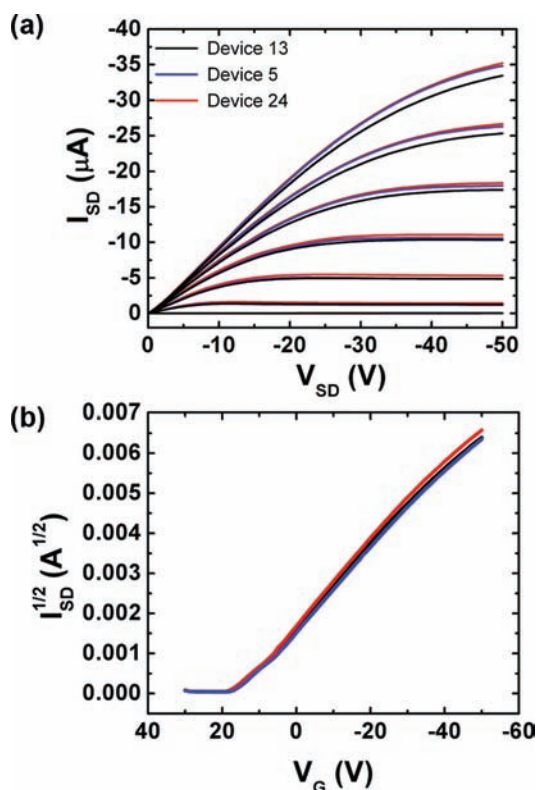


Figure 2. (a) Comparison of output curves for devices 13, 5, and 24 shown in Figure 1. The gate voltage, V_G , was increased from +10 to -50 V in steps of -10 V. (b) Transfer curves of the same devices shown in (a) collected at a source–drain voltage, V_{SD} , of -50 V.

active layer is independent of the alignment of the mean π -stacking direction along the ideal charge transport direction in these transistors. From the transfer curves in the saturation regime, we estimate the mobilities for all three devices to be $0.38 \text{ cm}^2/\text{V}\cdot\text{s}$. These results are in stark contrast to studies on transistors comprising rubrene and pentacene single crystals in

which at least a 2-fold difference in device mobility was observed depending on how the molecules are oriented with respect to the ideal charge transport direction in the active channels.^{2–7}

In all, we tested 46 devices on two different TES ADT spherulites to examine transistor performance as a function of molecular orientation. As can be seen from the polar plots shown in Figure 3, we observe no correlation between θ and (a) the device mobility, (b) the threshold voltage, V_T , or (c) the on/off ratio. The average mobility across all the devices is $0.37 \pm 0.03 \text{ cm}^2/\text{V}\cdot\text{s}$, corresponding closely to the value we previously predicted for the mobility of OFETs comprising single spherulites of TES ADT.⁹ The average V_T and on/off ratio are $22 \pm 4 \text{ V}$ and $(7 \pm 3) \times 10^3$, respectively. Though high, this V_T is comparable to what we had previously reported for OFETs with active channels comprising multiple spherulites of TES ADT;¹² this high V_T stems from moisture adsorption,¹⁷ as devices fabricated and tested in nitrogen consistently display V_T 's of $6 \pm 2 \text{ V}$.

While a direct comparison to mobilities derived from OFETs comprising single crystals of TES ADT would have been ideal, our efforts to make single-crystal TES ADT OFETs were hindered by the inability to make efficient electrical contact to rough TES ADT single crystals using “flip chip”⁷ or other soft-contact lamination¹⁸ techniques. Attempts to form large single crystals directly on dielectric surfaces comprising bottom-contact source and drain electrodes via drop casting or dip coating¹⁹ were also unsuccessful. Given that TES ADT crystallizes in the same brickwork-type packing motif as bis(triisopropylsilylethynyl) pentacene (TIPS pen),²⁰ and single crystals of TIPS pen display anisotropic photoconductivity along different crystallographic directions,⁶ it is not unreasonable to assume that charge transport anisotropy should also exist along different crystallographic directions of TES ADT. In fact, assuming the mobility anisotropy reported for rubrene single-crystal OFETs and accounting for a $\pm 20^\circ$ spread in molecular orientation distribution, we should still expect to see a 2-fold charge transport anisotropy in our devices.^{3,4} Further justification that TES ADT intraspherulite devices should show charge transport anisotropy stems from OFETs comprising needle-like crystals of solution-processed organic semiconductors that are unidirectionally crystallized under flow fields, in which charge transport is shown to be most efficient in the direction of maximum π -orbital overlap.¹⁹ That this charge transport anisotropy is absent in the active channels of TES ADT that exhibit preferential molecular orientation is thus surprising and implicates how sensitive

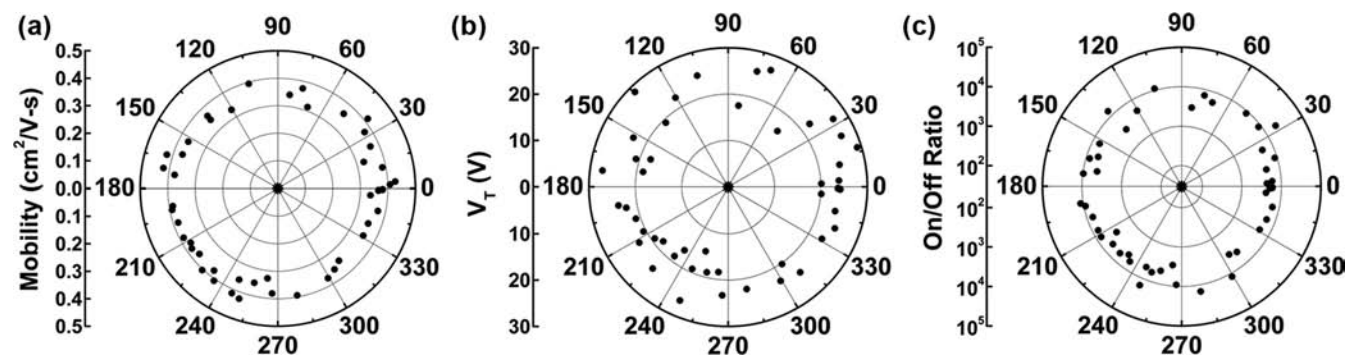


Figure 3. Polar plots of the (a) mobility, (b) V_T , and (c) on/off ratio of 46 devices as a function of θ .

macroscopic device performance is due to the presence microscopic structural heterogeneities.

To understand the origins of isotropic charge transport in intraspherulite TES ADT OFETs, we turn to a closer examination of the microstructure of these spherulites. Achieving a distribution of molecular orientations about the radial axis necessitates the formation of many low-angle grain boundaries within a single spherulite. We speculate that even small misalignments of molecules at these boundaries can lead to shallow traps, which in turn can limit charge transport. This conjecture is consistent with a recent report in which Podzorov and co-workers observed the absence of charge transport anisotropy along the different crystallographic directions of single-crystal rubrene at low temperatures, to which they ascribe shallow traps due to structural disorder.²¹ While it is commonly believed that charge transport is minimally affected by the presence of low-angle grain boundaries,²² the study presented herein clearly indicates otherwise.

In this manuscript, we report a systematic study on intraspherulite charge transport in solution-processed organic semiconductor thin films. In contrast to studies on single crystals, we find that charge transport within a TES ADT spherulite is independent of the mean π -stacking direction with respect to the channel length given the distribution of molecular orientations intrinsically sampled by spherulitic growth. While these structural heterogeneities that exist within solution-processed active layers are unavoidable consequences of rapid and inexpensive deposition techniques, they do not have to be detrimental to device performance. Rather, they can be exploited to promote uniformity in charge transport over large areas. As a point of comparison, the coefficient of variation (the standard deviation normalized by the mean) of mobilities extracted from intraspherulite TES ADT OFETs is almost an order of magnitude lower than those of mobilities extracted from OFETs comprising TES ADT prior to solvent-vapor annealing¹² and TIPS pen.²³ This substantially reduced variation in device performance among neighboring OFETs over meaningful macroscopic distances will allow us to overcome a significant bottleneck to commercialization.

AUTHOR INFORMATION

Corresponding Author

lloo@princeton.edu

Notes

The authors declare no competing financial interest.

ACKNOWLEDGMENTS

We acknowledge support from the NSF MRSEC program through the Princeton Center for Complex Materials (Grant DMR-0819860). This research was also supported by SOLAR-NSF (DMR-1035217). S.S.L. is supported by a National Defense Science and Engineering Graduate fellowship.

REFERENCES

- (1) de Boer, R. W. I.; Gershenson, M. E.; Morpurgo, A. F.; Podzorov, V. *Phys. Status Solidi A* **2004**, *201*, 1302. Gershenson, M. E.; Podzorov, V.; Morpurgo, A. F. *Rev. Mod. Phys.* **2006**, *78*, 973.
- (2) Lee, J. Y.; Roth, S.; Park, Y. W. *Appl. Phys. Lett.* **2006**, *88*, 252106.
- (3) Reese, C.; Bao, Z. *Adv. Mater.* **2007**, *19*, 4535.
- (4) Sundar, V. C.; Zaumseil, J.; Podzorov, V.; Menard, E.; Willett, R. L.; Someya, T.; Gershenson, M. E.; Rogers, J. A. *Science* **2004**, *303*, 1644.

- (5) Zeis, R.; Besnard, C.; Siegrist, T.; Schlockermann, C.; Chi, X.; Kloc, C. *Chem. Mater.* **2005**, *18*, 244.
- (6) Ostroverkhova, O.; Cooke, D. G.; Hegmann, F. A.; Tykewski, R. R.; Parkin, S. R.; Anthony, J. E. *Appl. Phys. Lett.* **2006**, *89*, 192113.
- (7) Goldmann, C.; Haas, S.; Krellner, C.; Pernstich, K. P.; Gundlach, D. J.; Batlogg, B. *J. Appl. Phys.* **2004**, *96*, 2080.
- (8) Li, Y.; Wu, Y.; Liu, P.; Prostran, Z.; Gardner, S.; Ong, B. S. *Chem. Mater.* **2006**, *19*, 418. Gawrys, P.; Boudinet, D.; Zagorska, M.; Djurado, D.; Verilhac, J.-M.; Horowitz, G.; Pécaud, J.; Pouget, S.; Pron, A. *Synth. Met.* **2009**, *159*, 1478. Lloyd, M. T.; Anthony, J. E.; Malliaras, G. G. *Mater. Today* **2007**, *10*, 34. Usta, H.; Risko, C.; Wang, Z.; Huang, H.; Delimeroglu, M. K.; Zhukhovitskiy, A.; Facchetti, A.; Marks, T. J. *J. Am. Chem. Soc.* **2009**, *131*, 5586.
- (9) Lee, S. S.; Kim, C. S.; Gomez, E. D.; Purushothaman, B.; Toney, M. F.; Wang, C.; Hexemer, A.; Anthony, J. E.; Loo, Y.-L. *Adv. Mater.* **2009**, *21*, 3605.
- (10) Lee, S. S.; Loo, Y.-L. *Annu. Rev. Chem. Biomol. Eng.* **2010**, *1*, 59.
- (11) Keith, H. D.; Padden, F. J. *J. Appl. Phys.* **1963**, *34*, 2409.
- (12) Dickey, K. C.; Anthony, J. E.; Loo, Y.-L. *Adv. Mater.* **2006**, *18*, 1721.
- (13) Lee, S. S.; Tang, S.; Smilgies, D.-M.; Woll, A. R.; Mativetsky, J. M.; Loth, M. A.; Anthony, J. E.; Loo, Y.-L. Submitted.
- (14) Dickey, K. C.; Smith, T. J.; Stevenson, K. J.; Subramanian, S.; Anthony, J. E.; Loo, Y.-L. *Chem. Mater.* **2007**, *19*, 5210.
- (15) Dickey, K. C.; Subramanian, S.; Anthony, J. E.; Han, L.-H.; Chen, S.; Loo, Y.-L. *Appl. Phys. Lett.* **2007**, *90*, 244103.
- (16) Jimison, L. H.; Toney, M. F.; McCulloch, I.; Heeney, M.; Salleo, A. *Adv. Mater.* **2009**, *21*, 1568.
- (17) Ye, R.; Baba, M.; Suzuki, K.; Ohishi, Y.; Mori, K. *Thin Solid Films* **2004**, *464–465*, 437. Majewski, L. A.; Kingsley, J. W.; Balocco, C.; Song, A. M. *Appl. Phys. Lett.* **2006**, *88*, 222108.
- (18) Kim, J. B.; Lee, S.; Toney, M. F.; Chen, Z.; Facchetti, A.; Kim, Y. S.; Loo, Y.-L. *Chem. Mater.* **2010**, *22*, 4931.
- (19) Sele, C. W.; Kjellander, B. K. C.; Niesen, B.; Thornton, M. J.; van der Putten, J. B. P. H.; Myny, K.; Wondergem, H. J.; Moser, A.; Resel, R.; van Breemen, A. J. J. M.; van Aerle, N.; Heremans, P.; Anthony, J. E.; Gelinck, G. H. *Adv. Mater.* **2009**, *21*, 4926. Headrick, R. L.; Wo, S.; Sansoz, F.; Anthony, J. E. *Appl. Phys. Lett.* **2008**, *92*, 063302.
- (20) Anthony, J. E.; Brooks, J. S.; Eaton, D. L.; Parkin, S. R. *J. Am. Chem. Soc.* **2001**, *123*, 9482. Payne, M. M.; Odon, S. A.; Parkin, S. R.; Anthony, J. E. *Org. Lett.* **2004**, *6*, 3325.
- (21) Podzorov, V.; Menard, E.; Borissov, A.; Kiryukhin, V.; Rogers, J. A.; Gershenson, M. E. *Phys. Rev. Lett.* **2004**, *93*, 086602.
- (22) Street, R. A.; Northrup, J. E.; Salleo, A. *Phys. Rev. B* **2005**, *71*, 165202.
- (23) Park, S. K.; Jackson, T. N.; Anthony, J. E.; Mourey, D. A. *Appl. Phys. Lett.* **2007**, *91*, 063514.